

Original Research

Size Control of Cobalt Oxide Nanoparticles and Its Effect on the Fenton Catalytic Activity

Elvera L. Viljoen*, Semakaleng V. Kganyago, Augustine E. Ofomaja

Vaal University of Technology, Private Bag x021 Vanderbijlpark, 1900, South Africa

Received: 8 January 2020

Accepted: 5 April 2020

Abstract

Cobalt oxide nanoparticles were prepared using a precipitation-oxidation method at mild reaction conditions. The nanoparticles had spherical shapes and sizes that ranged from 4.6 nm to 19.4 nm as determined by TEM and XRD. XRD indicated that the nanoparticles consisted only of the Co_3O_4 phase. The nanoparticles' size was controlled using different amounts of the oxidant, hydrogen peroxide. The size was controlled in the absence of capping molecules. The yield increased with an increase in the amount of hydrogen peroxide used. The cobalt oxide nanoparticles were used as catalyst for the Fenton reaction to degrade methylene blue dye by hydrogen peroxide oxidation. The catalytic activity increased with a decrease in particle size. A percentage degradation of 99 % in 30 minutes was obtained when the 4.6 nm sized nanoparticles was used as catalyst. No significant methylene blue degradation was observed in the absence of the catalyst.

Keywords: nanoparticles, Fenton, catalysis, water remediation, effect of size

Introduction

The pollution of the world's limited water resources is becoming an increasingly difficult challenge. Therefore, it is important to develop processes to remediate polluted water. Organic pollutants that are aromatic in nature are resistant to natural biodegradation mechanisms. These pollutants originate from chemical industries, pharmaceutical companies and pesticides used in agriculture. Advanced oxidation processes (AOP) can be used to degrade these recalcitrant organic pollutants through chemical oxidation. Examples

of AOP are the Fenton reaction, ozonation, and photocatalysis. In this study methylene blue dye was used as a model aromatic organic pollutant.

The Fenton reaction is catalysed by transition metal oxides such as iron oxide, copper oxide and cobalt oxide. Heterogenous catalysts are preferred for commercial application to the originally used homogenous iron ions, due to the easier separation of heterogenous catalysts from the water.

Espinoza et al. [1] showed that smaller iron oxide nanoparticles supported on diamond are more active than larger particles for photo-Fenton catalysis. Dong et al. [2] tested unsupported cobalt oxide particles with sizes of 3.5 nm, 19 nm and 70 nm and showed that the rate of oxidation degradation of phenol by ozone increases with a decrease in the unsupported

*e-mail: elverav@vut.ac.za

cobalt oxide particle size. Wan et al. [3] showed that the Fenton activity increased when unsupported iron oxide particles decreased from 600 nm to 30 nm. This increase in activity with a decrease in the particle size may be explained by an increase in the surface area with a corresponding decrease in the particle size. From a catalysis point of view, the investigation of sizes smaller than 20 nm is of more interest and deviations due to the small size have been found for other reactions like Fischer-Tropsch. For example, Bezemer et al. [4] found that the Fischer-Tropsch catalytic activity increased when the size was decreased from 27 nm to 6 nm but the activity decreased on further reduction of the cobalt particle size to 2.6 nm. This research indicated that there may be an optimum size to achieve the highest activity and that it thus is important to specifically test in the size range below 20 nm. No research has been found specifically on the size effect of cobalt oxide on the Fenton reaction in this size range.

In this study, the effect of the size of unsupported cobalt oxide nanoparticles were investigated. Unsupported, non-agglomerated nanoparticles have been chosen to study the effect of size in the absence of mass transfer limitations and metal oxide support interactions. Commercial catalysts are typically supported since supported metal oxide nanoparticles are easier to separate and supported catalysts are required for fixed bed operation to minimise pressure drop over the reactor. Commercial supports often have pore sizes smaller than 20 nm to maximize the surface area of the support. This leads to the formation of metal oxide particle sizes smaller than 20 nm when the metal oxide particle form inside the support pores [5]. Therefore, this study focused on particles sizes smaller than 20 nm and to obtain more information specifically in this region of interest from a commercial application point of view.

The preparation of cobalt oxide with different sizes is also of interest for non-catalytic applications such as batteries, gas-sensing and data storage. Other properties, apart from catalytic activity, like the current density, capacitive performance [6] and magnetic properties [7] are also influenced by the cobalt oxide particle size. For example, small sized cobalt oxide nanoparticles are ferromagnetic and when the size is increased, they become superparamagnetic [7].

There are various bottom-up methods, such as precipitation, hydrothermal, solvothermal, vapour deposition, and thermal decomposition, to prepare nanoparticles [8, 9]. Each preparation method has unique advantages and disadvantages over the alternative methods [8, 9]. The major disadvantage of hydrothermal and solvothermal is that a high pressure autoclave is required to heat the reaction mixture above the solvent boiling point [8, 9]. The advantage the simple precipitation oxidation method is that cobalt oxide nanoparticles can be prepared at low temperatures (<100°C) and atmospheric pressure thus simple glassware can be used. Solvothermal, physical and

chemical vapor deposition and thermal decomposition of metal complexes methods require solvents, capping molecules, surfactants or metal complexes that can be expensive, toxic and explosive [8, 9] which can be avoided if a simple precipitation oxidation method is used.

The cobalt oxide nanoparticles in this study have been prepared using a precipitation oxidation method. H_2O_2 oxidation was used to form Co_3O_4 at low temperatures instead of the more usual calcination in air, in order to prevent sintering [10]. This method has been selected since large enough quantities of nanoparticles can be prepared which is required for catalytic testing. Capping molecules are often used for size and shape control of nanoparticles. In this study, the cobalt oxide nanoparticles were specifically prepared in the absence of complex organic capping molecules since capping molecules are expected to be adsorbed on the surface, leading to a decrease in the catalytic activity by blocking the catalytic sites. Previously it has been reported that the sizes of the nanoparticles can be controlled by using different amounts of hydrogen peroxide [10, 11]. An increase in the molar ratio of H_2O_2 to Co^{2+} from 4:1 to 20:1 was reported to result in an increase in the Co_3O_4 nanoparticle size from about 18 nm to about 27 nm [10]. In contrast, the increase of the H_2O_2 to Co^{2+} molar ratio from 1:1 to 3:1 resulted in a decrease in the size of the obtained Co_3O_4 nanoparticles from ~300 nm to ~30 nm [11]. The effect of H_2O_2 may be related to the molar ratio of H_2O_2 to Co^{2+} as well as the preparation method used. It can be argued that at low H_2O_2 to Co^{2+} molar ratio the size decreases and at higher H_2O_2 to Co^{2+} molar ratio the size increases. No prior research has been found where the H_2O_2 amount has been used to control the cobalt oxide nanoparticle size in the range 5 to 20 nm.

Theoretically, a molar ratio of H_2O_2 to Co^{2+} of 0.33:1 is required to form Co_3O_4 . Research has shown that a much higher amount than the theoretical amount is required to form only Co_3O_4 . Yang et al. [12] indicated that experimentally an excess of hydrogen peroxide is required (H_2O_2 to Co^{2+} above 2.5:1.0), which they attributed to the decomposition of H_2O_2 . Amiri et al. [10] utilized a much larger excess of hydrogen peroxide with a molar ratio of H_2O_2 to Co^{2+} of 20:1 (assuming a H_2O_2 concentration of 30%). An increase in the excess of oxidant added to the synthesis mixture resulted in a decrease in cobalt hydroxide and increasing the yield of Co_3O_4 nano-particles [12]. A high reaction temperature of 150°C or higher is also required to minimize the amount of cobalt hydroxide like species and to form only Co_3O_4 [13, 14]. In this study a low molar ratio of H_2O_2 to Co^{2+} at a relatively low temperature was used which is expected to result in a mixture of cobalt hydroxide, cobalt hydroxide nitrate species and Co_3O_4 . A purification step is thus required to remove these species. Pure Co_3O_4 can be obtained from these solid mixtures by suspending the solid in dilute hydrochloric

acid solutions resulting in the selective dissolution of these hydroxide species [15].

The objective of this study was to develop a simple low temperature, atmospheric pressure, nanoparticles preparation method without capping molecules using H_2O_2 to control the size between 5 and 20 nm and to obtain a high yield of pure Co_3O_4 . These nanoparticles were subsequently used to study the influence of cobalt oxide nanoparticle size on the Fenton catalytic activity.

Materials and Methods

Materials

Cobalt nitrate hexahydrate, $(Co(NO_3)_2 \cdot 6H_2O)$, (98%), and sodium hydroxide, (NaOH, 98%) were purchased from Sigma-Aldrich. Hydrogen peroxide (H_2O_2 in water, 30%), hydrochloric acid, (HCl 32%) and methanol, (CH_3OH , 99%) were purchased from Glassworld. Butanol, ($C_4H_{10}O$, 99.8%) was obtained from Laboratory Consumables. All chemicals were used as received, without further purification.

Preparation of Co_3O_4 Nanoparticles

Cobalt nitrate hexahydrate (5.8178 g) was dissolved in 10 mL of distilled water and a solution of hydrogen peroxide (2.9 mmol) dissolved in 10 mL of distilled water were mixed together at room temperature. Sodium hydroxide (1.2743 g) was dissolved in 100 mL of distilled water. The mixture of cobalt nitrate/hydrogen peroxide and n-butanol (20 mL) were added to the solution of sodium hydroxide; the mixture turned brown/black. The solution contained in a round bottom flask was placed in an unheated heating mantle and heated up to 85°C. The mixture was kept at 85°C for 16 hours while continuously bubbling air and stirring with a magnetic stirrer at 300 rpm. The solution was allowed to cool to room temperature and centrifuged at 5000 rpm for 5 minutes. The solid product was washed three times with 50 mL 2M HCl aliquots to dissolve the unreacted cobalt hydroxide, twice with 50 mL of distilled water to remove the HCl and finally, once with 50 mL of methanol to remove water. The nanoparticles produced were left to dry in an oven at 120°C overnight. The same procedure was followed subsequently, by only changing the amount of hydrogen peroxide used (2.9, 1.4, 0.74, 0.37, 0.14 mmol H_2O_2).

Characterization

XRD analyses were done using the Shimadzu-XRD 700, X-Ray Diffractometer with Cu K α radiation ($\lambda = 1.154056 \text{ \AA}$). A scan speed of 1°/minute, current of 30 mA and a voltage of 40 kV were used. The FWHM (Full-Width Half-Maximum) was determined by fitting a Gaussian peak using the Fityk™ peak fitting programme. The FWHM was used to calculate the

average crystallite size using the Scherrer equation as shown in Equation 1.

$$D = K\lambda/\beta\cos\theta \quad (1)$$

A value of 0.9 was used for the Scherrer constant K , 1.154056 \AA for λ , β is the line width FWHM as 2θ , θ is the Bragg angle, and D is the crystallite size. The strongest diffraction peak, (311), at $\sim 36^\circ 2\theta$ were used to calculate the average crystallite size. UV-VIS spectroscopy analyses were performed with a double beam spectrometer – a Perkin Elmer Lambda 25 UV-VIS spectrometer, with a tungsten and deuterium lamp, using a bandwidth of 1 nm with a fixed slit. A baseline setting was conducted by using pure water as a reference sample. A very small amount of the solid sample/crystals was dispersed in water. A Gaussian peak was fitted to the adsorption peak with the program Fityk™ to obtain the peak maximum position. The size and shape of the dried unsupported nanoparticles were determined using a TEM, LEO TEM 912, with an acceleration voltage of 120 kV and a tungsten wire filament. The nanoparticles dispersed in the methanol were pipetted onto carbon coated, copper grids and allowed to dry. The nanoparticles' sizes were measured using the software programme; ImageJ™.

Fenton Degradation Tests

Reactions were carried out in a 250 mL beaker covered with aluminium foil to avoid photo-degradation. A volume of 10 mL of methylene blue stock solution (1000 ppm) and 20 mL of distilled water were mixed. A mass of 0.01 g of catalyst was dispersed in 50 mL of distilled water and sonicated for 30 minutes using an ultrasonic bath. The catalyst was added to the solution of methylene blue. The mixture was stirred for 1 hour in order reach adsorption equilibrium of the methylene blue on the catalyst surface. The Fenton reaction is initiated with the addition of 20 mL of 30% H_2O_2 . Small-sized samples (1 mL) were taken periodically. Isopropanol (1 mL) was added to the sample to stop the reaction by quenching the OH radicals. Then the solution was diluted to the mark with cold distilled water in 100 mL volumetric flask. The sample solution was centrifuged to remove the solid catalyst particles from the liquid phase. The concentration of methylene blue was determined with UV-VIS spectroscopy at a wavelength of 660 nm.

Results and Discussion

Catalyst Characterization

X-ray Diffraction (XRD) results showed that the cubic phase Co_3O_4 (JCPDS data, PDF card No.00-04-1003) was obtained for all the samples. No other diffraction peaks were observed in the XRD

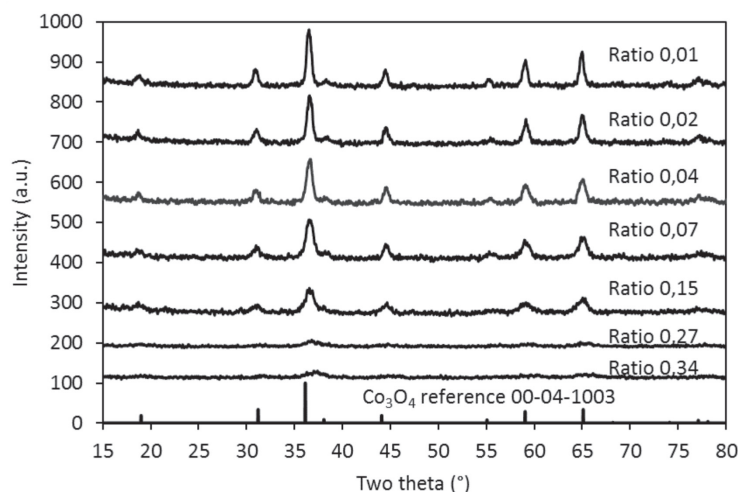
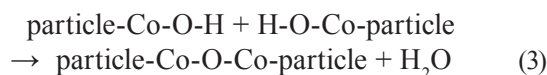
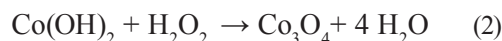


Fig. 1. X-ray Diffraction pattern of the Co_3O_4 nanoparticles prepared at 85°C for 16 hrs.

spectra such as cobalt hydroxide indicating that the purification technique with diluted hydrochloric acid dissolved the cobalt hydroxide-like species. The diffraction peaks became broader with an increase in the H_2O_2 to Co^{2+} mol ratio indicating that the cobalt

oxide crystallite size decreased with an increase in the H_2O_2 to Co^{2+} molar ratio (see Fig. 1). The size of the cobalt oxide crystallites was calculated using the Scherrer equation (see Fig. 3) which indicated that the crystallite size decreased from 14 nm to about 5 nm when the H_2O_2 to Co^{2+} molar ratio increased from 0.01 to 0.34. TEM analyses indicated a similar trend to the XRD analyses and showed that an increase in the H_2O_2 to Co^{2+} molar ratio decreased the corresponding sizes of the Co_3O_4 nanoparticles (see Figs 2 and 3). This may be explained by the formation of more Co_3O_4 nuclei due to faster oxidation by the higher concentrations of H_2O_2 . The particle size distribution (standard deviation) also decreased with an increase in the H_2O_2 to Co^{2+} molar ratio. The yield of the Co_3O_4 nanoparticles increased with an increase in the H_2O_2 amount (see Fig. 3) which is in agreement with literature [12]. The higher yield may be explained by a higher conversion of cobalt hydroxide to Co_3O_4 by oxolation which is a condensation type of reaction resulting in the formation of oxo bridges as shown in Equation 2 and 3 [12, 16, 17].



The size of the smaller particles calculated using XRD results were found to be slightly larger than those obtained from TEM (see Table 2 and Fig. 4) and this slight difference might be due to the presence of a few larger nanoparticles that were not seen in the TEM images. The larger particles' XRD sizes were smaller than the size determined by TEM which may be explained by the particles containing some faults and cracks which is visible in some of the particles as seen in the TEM photographs.

TEM analysis showed that Co_3O_4 nanoparticles have mostly spherical shapes (see Fig. 3) for a H_2O_2 to Co^{2+}

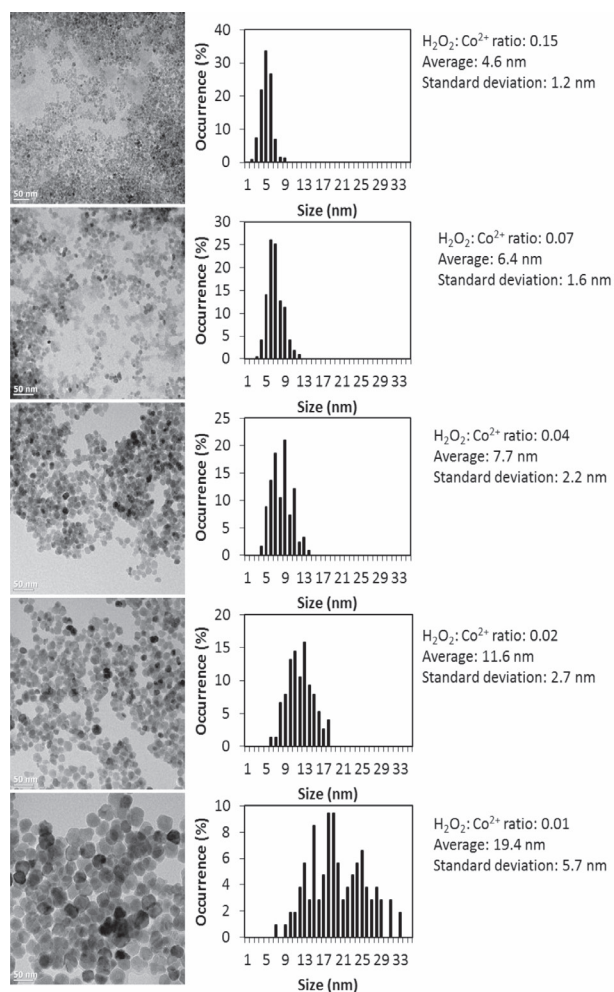


Fig. 2. TEM analyses of Co_3O_4 nanoparticles.

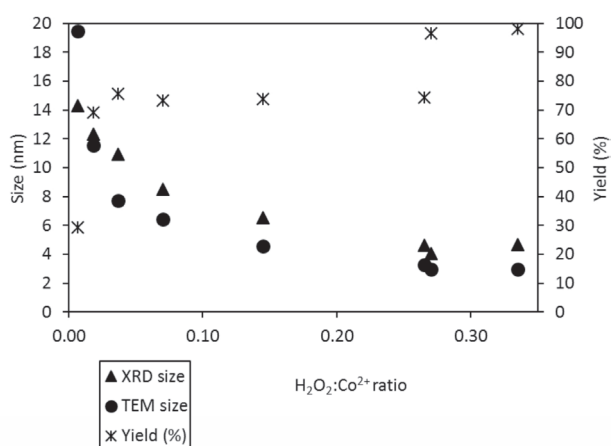


Fig. 3. Effect of the $\text{H}_2\text{O}_2:\text{Co}^{2+}$ molar ratio on the Co_3O_4 yield and nanoparticles sizes as determined by TEM and XRD.

molar ratio between 0.02 and 0.15. More particles with sharp edges were observed when the H_2O_2 to Co^{2+} molar ratio was decreased. The shape may be changing from spherical to hexagonal or cubic. The rate of conversion of the cobalt hydroxide to the Co_3O_4 phase may have been slower at the lower $\text{H}_2\text{O}_2:\text{Co}^{2+}$ molar ratio resulting in thermodynamically controlled growth [18] rather than kinetically controlled growth of the cobalt oxide crystallites. Thermodynamically controlled growth will lead to the formation of thermodynamically more stable surfaces such as the $\{100\}$ crystal facet which has the lowest surface energy for the Co_3O_4 phase [19]. The $\{100\}$ crystal facets will lead to a cubic shaped nanoparticle.

At a H_2O_2 to Co^{2+} molar ratios of 0.27 and 0.34, the TEM analyses showed that the nanoparticles were agglomerated and not well defined and the XRD diffraction peaks were broad indicating that the crystallites are small and amorphous. The reported sizes in Fig. 3 for the nanoparticles prepared at H_2O_2 to Co^{2+} molar ratios of 0.27 and 0.34, are rough estimates.

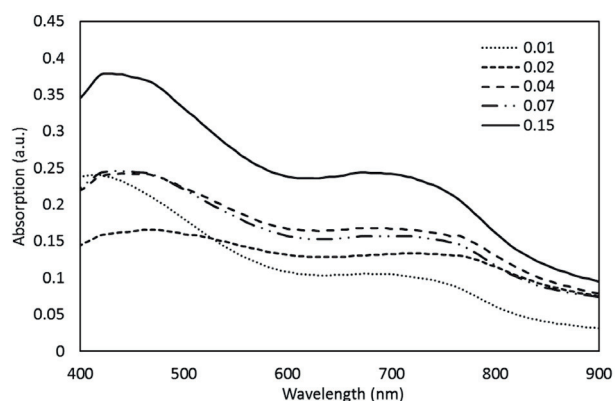


Fig. 4. UV-VIS spectra of the cobalt oxide nanoparticles suspended in water.

The optical properties were investigated by UV-VIS spectroscopy as shown in Fig. 4. The two absorption peaks observed at wavelength around 750 nm and 450 nm (see Fig. 4) are assigned to ligand to metal charge transfers of $\text{O}^{2-}\rightarrow\text{Co}^{3+}$ and $\text{O}^{2-}\rightarrow\text{Co}^{2+}$ since the Co_3O_4 phase contains two cobalt ion oxidation states, Co(II) and Co(III) [20]. The wavelength of the peak maximum of the Co_3O_4 nanoparticles increased when the particle size increased from 4.6 nm to 11.6 nm as shown in Fig. 5. This indicates that the band gap increased with a decrease in the particle size from 4.6 nm to 11.6 nm, which is in line with that reported in literature [20-22]. The band gap of the 19.4 nm particles was similar to the 4.6 nm particles (see Fig. 5). Not only the nanoparticles' size, but also their shape has an influence on the optical properties of metal oxides [21]. The TEM of the 19.4 nm particles shows that they are not spherical, but with flat edges and cracks. This shape change may explain the lower wavelength of the peak maxima obtained for the 19.4 nm particles.

Co_3O_4 can also be used as a photocatalyst for the degradation of organic pollutants [23, 7]. The catalytic activity of a photocatalyst is influenced by the band gap of photocatalyst and surface area which is related to the particle size [23, 7]. The optical properties become an important characteristic when the catalyst is used as a photocatalysis instead of Fenton catalysis since photocatalysis requires the excitation of an electron from the valence band to the conduction band by the adsorption of light [7, 24, 25]. Adsorption in visible light and a small band gap is preferred because solar light consists mostly of visible light. The blue shift of the adsorption peak due to a decrease in the cobalt nanoparticles size as shown in Fig. 4, indicating an increase in the band gap, may possibly decrease the visible light photocatalytic activity even though the catalytic surface area has increased.

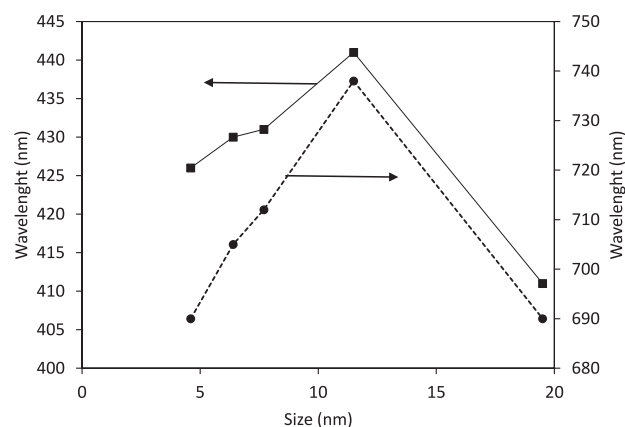


Fig. 5. Influence of the cobalt nanoparticle size on the peak maximum wavelengths.

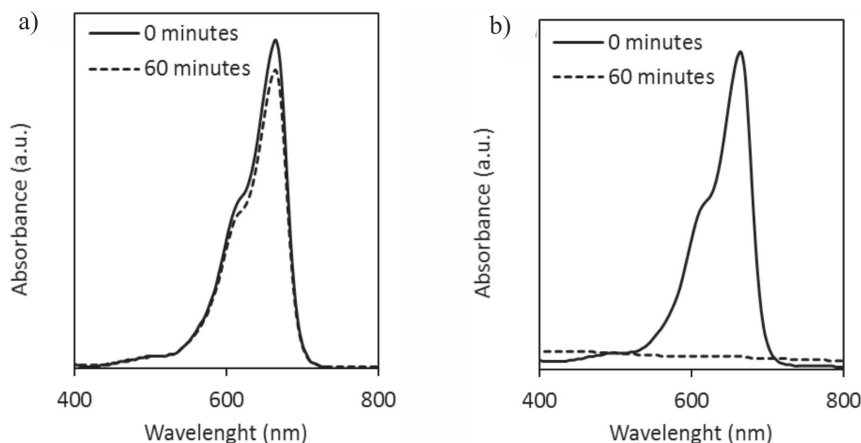
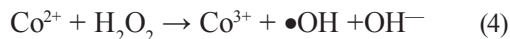


Fig. 6. Degradation of methylene blue a) without and b) with Co_3O_4 nanoparticles.

Catalytic Activity of Co_3O_4 Nanoparticles on the Degradation of Methylene Blue Dye

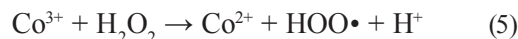
The ability of H_2O_2 to degrade methylene blue in the absence of a catalyst was evaluated as shown in Fig. 6a). The intense absorption peak at 660 nm was still observed even after 60 min reaction which means that a negligible amount of degradation of methylene blue took place which may be explained by the low oxidation potential of H_2O_2 compared with OH radicals. The addition of the catalyst resulted in the degradation of the methylene blue (Fig. 6b) which indicates that the catalyst is thus required to produce OH radicals by the Fenton reactions as shown in Equation 4.



An induction time of about 10 minutes was observed as shown in Fig. 7. Induction periods have also been observed for other Fenton catalytic systems [26, 27] and have been explained by a time-dependent activation process by dissolution of the metal ions or the protonation of the surface species since lowering the pH decreases the induction period.

The rate of catalytical degradation of methylene blue increase with a decrease in the Co_3O_4 nanoparticle sizes as depicted in Fig. 7a). The degradation reaction was first order in methylene blue as shown in Fig. 7b). This observation agrees with previous research for the Fenton and ozonation oxidation degradation reactions [1, 2, 3]. However, an optimum size was not observed for the Fenton reaction as reported for the Fischer-Tropsch reaction [4], which indicates that when preparing a commercial supported catalyst one can aim to make a catalyst with the smallest crystallite size. The metal support interaction, which is typically present for very small metal oxide nanoparticles, will not influence the catalytic activity. Strong metal support interaction may influence the reducibility of the metal oxide and may decrease the rate of reduction of the Co^{3+} back to Co^{2+} as shown in Equation 5. The influence

of the support needs to be considered when preparing supported catalysts.



The advantage of using a support is that it prevents the nanoparticles from agglomerating since not only the size but also on the amount of agglomeration affects the activity [28]. The use of mesoporous silica as support increased the activity of Co_3O_4 nanoparticles which had a size of 23 nm [29].

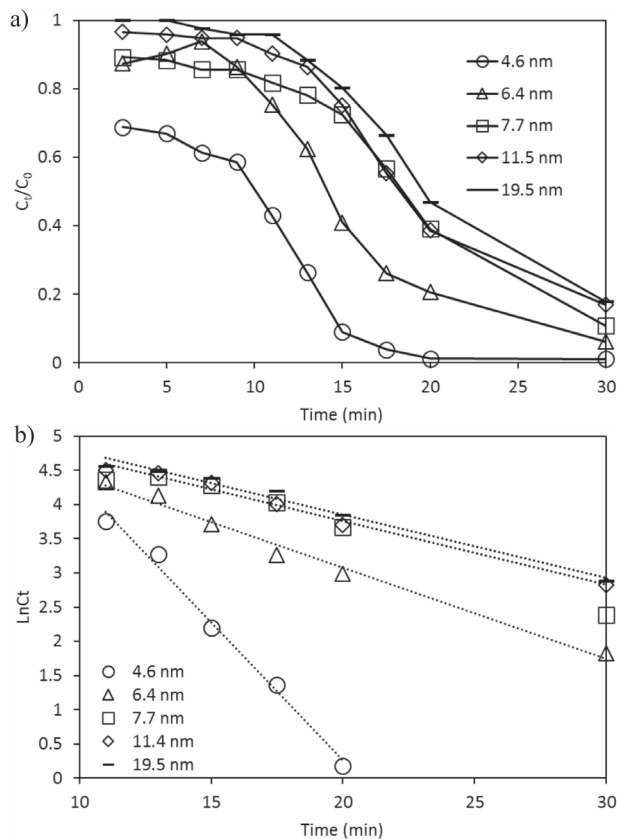


Fig. 7. Methylene blue degradation using cobalt oxide nanoparticles with different sizes as catalysts.

In would be interesting to test the effect of the Co_3O_4 crystallite size on the photocatalytic activity since an increase in the rate constant was observed for an increase in the crystallite size of CoFe_2O_4 from 13.4 nm to 29.1 nm [22] which is in contrast to the finding in this study which may be explained by the photocatalysis activity being influenced by both the band gap and the surface area where as the Fenton catalysis only depends on the surface area. Both the band gap and the surface area are influenced by the size of the nanoparticles.

Conclusions

A facile precipitation-oxidation method was developed to prepare Co_3O_4 nanoparticles of different sizes at atmospheric pressure and low temperature, without the use of complex organic capping agents. The size of Co_3O_4 nanoparticles was controlled by different amounts of H_2O_2 and a decrease in particle size was observed with an increase in the amount of H_2O_2 added. An insignificant amount of degradation took place in the absence of the Co_3O_4 nanoparticles indicating the necessity of a catalyst in order for the Fenton reaction to proceed. The catalytic activity of the Co_3O_4 nanoparticles increased with a decrease in size from 19.5 to 4.6 nm. A percentage degradation of 99 % in 30 minutes was obtained when the Co_3O_4 nanoparticles of 4.6 nm were used as catalyst. The enhanced catalytic activity from the smallest nanoparticles may be explained in that the nanoparticles with smaller sizes have a higher surface area yielding more catalytically active sites. The results suggest that when preparing commercial catalysts, one should aim for the smallest possible metal oxide particle sizes to optimize the Fenton catalytic activity.

Acknowledgements

This work was based on the research supported by the National Research Foundation of South Africa from the grant, Unique Grant No. 99330, with additional funding from the Sasol University Collaboration Program and from the Vaal University of Technology. The authors express their thanks and appreciation to these institutions.

Conflict of Interest

The authors declare no conflict of interest.

References

1. ESPINOSA J.C., CATALÁ C., NAVALÓN S., FERRER B., ÁLVARO M., GARCÍA H. Iron oxide nanoparticles supported on diamond nanoparticles as efficient and stable catalyst for the visible light assisted Fenton reaction. *Appl. Catal. B: Environmental*. **226**, 242, **2018**.
2. DONG Y., HE K., YIN L., ZHANG A. A facile route to controlled synthesis of Co_3O_4 nanoparticles and their environmental catalytic properties. *Nanotechnology*. **18** (43), 435602, **2007**.
3. WAN D., LI W., WANG G., WEI X. Size-controllable synthesis of Fe_3O_4 nanoparticles through oxidation-precipitation method as heterogeneous Fenton catalyst. *J. Mater. Res.* **31** (17), 2608, **2016**.
4. BEZEMER G.L., BITTER J.H., KUIPERS H.P.C.E., OOSTERBEEK H., HOLEWIJN J.E., XU X., KAPTEIJN F., VAN DIJLEN A., JONG K.P. Cobalt Particle Size Effects in the Fischer - Tropsch Reaction Studied with Carbon Nanofiber Supported Catalysts. *J. Am. Chem. Soc.* **128** (6), 3956, **2006**.
5. CHENG K., VIRGINIE M., ORDOMSKY V.V., CORDIER C., CHERNAVSKII P.A., IVANTSOV M.I., PAUL S., WANG Y., KHODAKOV A.Y. Pore size effects in high-temperature Fischer - Tropsch synthesis over supported iron catalysts. *J. Catal.* **328**, 139, **2015**.
6. ZHOU F., LIU Q., GU J., ZHANG W., ZHANG D. A facile low-temperature synthesis of highly distributed and size-tunable cobalt oxide nanoparticles anchored on activated carbon for supercapacitors. *J. Power Sources*. **273**, 945, **2015**.
7. PARHIZKAR J., HABIBI M.H. Investigation and Comparison of Cobalt ferrite composite nanoparticles with individual iron oxide and cobalt oxide nanoparticles in azo dyes removal, *J. Water Environ. Nanotechnol.* **4** (1), 17, **2019**.
8. NIKAM A.V., PRASAD B.L.V., KULKARNI A.A. Wet chemical synthesis of metal oxide nanoparticles: A review. *CrystEngComm*. **20** (35), 5091, **2018**.
9. JAMKHANDE P.G., GHULE N.W., BAMER A.H., KALASKAR M.G. Metal nanoparticles synthesis: An overview on methods of preparation, advantages and disadvantages, and applications. *J. Drug Deliv Sci Technol.* **53**, 101174, **2019**.
10. HASHEMI AMIRI S.E., VAEZI M.R., ESMAIELZADEH KANDJANI A. A comparison between hydrothermally prepared Co_3O_4 via H_2O_2 assisted and calcination methods. *J. Ceram. Process. Res.* **12** (3), 327, **2011**.
11. SONG X.C., WANG X., ZHENG Y.F., MA R., YIN H.Y. Synthesis and electrocatalytic activities of Co_3O_4 nanocubes. *J. Nanopart. Res.* **13** (3), 1319, **2011**.
12. YANG Y. PING, HUANG K. LONG, LIU R. SHENG, WANG L. PING, ZENG W. WEN, ZHANG P. MIN. Shape-controlled synthesis of nanocubic Co_3O_4 by hydrothermal oxidation method. *Transactions of Nonferrous Metals Society of China (English Edition)*. **17** (5), 1082, **2007**.
13. JIANG Y., WU Y., XIE B., XIE Y., QIAN Y. Moderate temperature synthesis of nanocrystalline Co_3O_4 via gel hydrothermal oxidation. *Mater. Chem. Phys.* **74** (2), 234, **2002**.
14. ZHANG Y., LIU Y., FU S., GUO F., QIAN Y. Morphology-controlled synthesis of Co_3O_4 crystals by soft chemical method. *Mater. Chem. Phys.* **104** (1), 166, **2007**.
15. FENG J., ZENG H.C. Size-Controlled Growth of Co_3O_4 Nanocubes. *Chem. Mater.* **15** (14), 2829, **2003**.
16. BAUMGARTNER J., DEY A., BOMANS P.H.H., LE COADOU C., FRATZL P., SOMMERDIJK N.A.J.M., FAIVRE D. Nucleation and growth of magnetite from solution. *Nat. Mater.* **12** (4), 310, **2013**.

17. JOLIVET J.P., TRONC E., CHANÉAC C. Iron oxides: From molecular clusters to solid. A nice example of chemical versatility. *Comptes Rendus – Geoscience*. **338** (6-7), 488, **2006**.
18. HE T., CHEN D., JIAO X., WANG Y., DUAN Y. Solubility-Controlled Synthesis of High-Quality Co_3O_4 Nanocrystals. *Chem. Mater.* **17**, 4023, **2005**.
19. SU W., DOU S., WANG G. Single Crystalline Co_3O_4 Nanocrystals Exposed with Different Crystal Planes for Li-O_2 Batteries. *Scientific Reports*. **4**, 5767, **2014**.
20. SARFRAZ A.K., HASANAIN S.K. Size dependence of magnetic and optical properties of Co_3O_4 nanoparticles. *Acta Physica Polonica A*. **125** (1), 139, **2014**.
21. SINGH M., GOYAL M., DEVLAL K. Size and shape effects on the band gap of semiconductor compound nanomaterials. *J. Taibah Univ. Sci.* **12** (4), 470, **2018**.
22. ANNIE VINOSHA P., JEROME DAS S. Investigation on the role of pH for the structural, optical and magnetic properties of cobalt ferrite nanoparticles and its effect on the photo-fenton activity. *Materials Today: Proceedings*. **5** (2), 8662, **2018**.
23. EDLA R., PATEL N., EL KOURA Z., FERNANDES R., BAZZANELLA N., MIOTELLO A. Pulsed laser deposition of Co_3O_4 nanocatalysts for dye degradation and CO oxidation. *Appl. Surf. Sci.* **302**, 105, **2014**.
24. MORIDON S.N.F., SALEHMIN M.I., MOHAMED M.A., ARIFIN K., MINGGU L.J., KASSIM M.B. Cobalt oxide as photocatalyst for water splitting: Temperature-dependent phase structures. *Int. J. Hydrog. Energy*. **44** (47), 25495, **2019**.
25. MAGDALANE C.M., KAVIYARASU K., ARULARASU M.V., KANIMOZHI K., RAMALINGAM G. Structural and morphological properties of Co_3O_4 nanostructures: Investigation of low temperature oxidation for photocatalytic application for waste water treatment. *Surf. Interfaces*. **17**, 100369, **2019**.
26. ZHOU S., HU X., XU R., XIA C., ZHANG H., ZHANG C., WANG Y., SONG Z. Catalytic wet peroxide oxidation of 4-chlorophenol over Al-Fe-, Al-Cu-, and Al-Fe-Cu-pillared clays: Sensitivity, kinetics and mechanism. *Appl Clay Sci.* **95**, 275, **2014**.
27. XU L., WANG J. A heterogeneous Fenton-like system with nanoparticulate zero-valent iron for removal of 4-chloro-3-methyl phenol. *J. Hazard. Mater.* **186** (1), 256, **2011**.
28. VILJOEN E.L., THABEDE P.M., MOLOTO M.J., MUBIAYI K.P., DIKIZA B.W., AFRICA S. The influence of sodium hydroxide concentration on the phase, morphology and agglomeration of cobalt oxide nanoparticles and application as Fenton catalyst. *Dig. J. Nanomater. Biostructures*. **14** (4), 1131, **2019**.
29. DENG J., FENG S.F., ZHANG K., LI J., WANG H., ZHANG T., MA X. Heterogeneous activation of peroxymonosulfate using ordered mesoporous Co_3O_4 for the degradation of chloramphenicol at neutral pH. *Chem. Eng. J.* **308**, 505, **2017**.